Supporting Information

On-Chip Single-Layer Integration of Diamond Spins with Microwave and Plasmonic Channels

Mikhail Y. Shalaginov, Simeon I. Bogdanov, Alexei S. Lagutchev, Alexander V. Kildishev, Alexandra Boltasseva, and Vladimir M. Shalaev*

School of Electrical & Computer Engineering, Birck Nanotechnology Center, and Purdue Quantum Science & Engineering Institute, Purdue University, West Lafayette, IN 47907, USA

*Email: shaginov@purdue.edu

I. Optical properties of NV ensembles in a nanodiamond

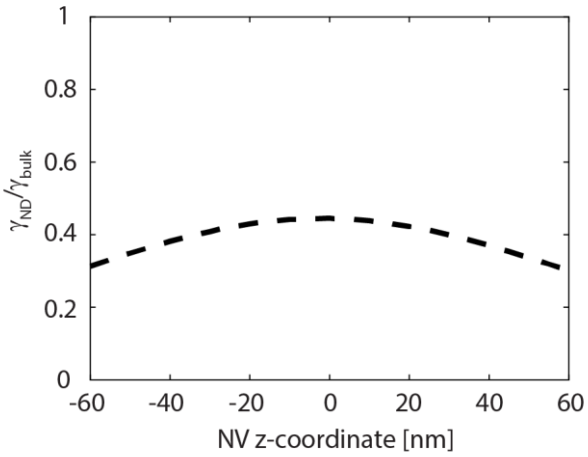

Figure S1. The ratio of the total decay rate of an NV inside a nanodiamond immersed in air (γ_{ND}) to γ_{bulk}.

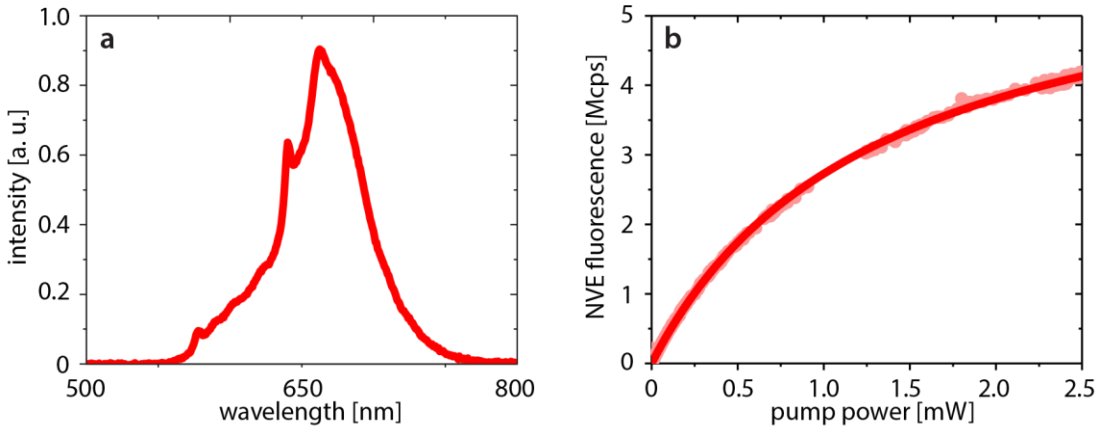

Figure S2. (a) Emission spectrum of NVE excited with a 532 nm laser. Peak wavelength is 663 nm. (b) Saturation dependence of NVE fluorescence vs laser pump power: extrapolated saturated fluorescence is 6.4 Mcps, saturation pump power is 1.3 mW. In spin readout measurements the excitation power was 15 μW.

II. Details of NVE spin contrast measurements

Continuous-wave ODMR

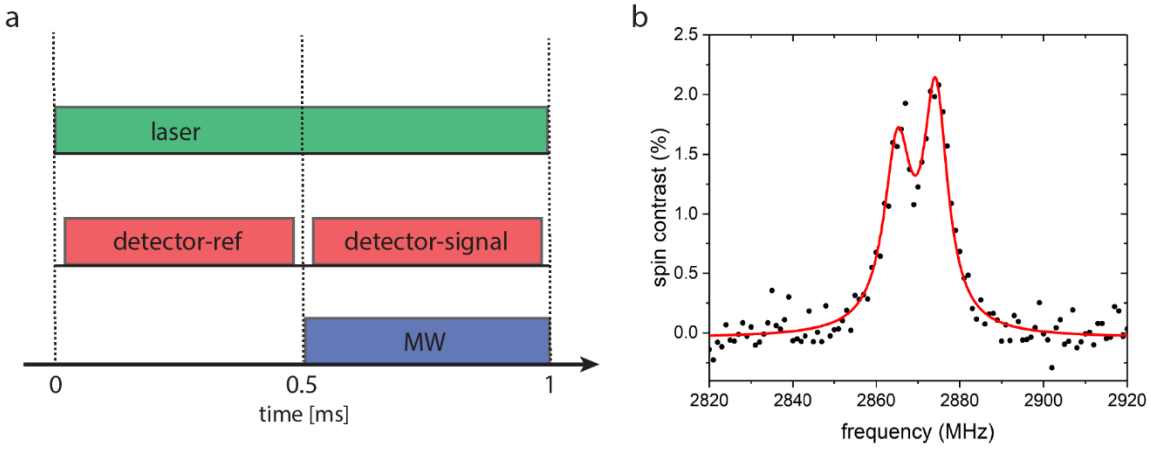

Figure S3. (a) CW ODMR measurement protocol. (b) Spin contrast curve obtained in a CW ODMR experiment with a 0.46 ms MW pulse at 8 dBm generator power.

The cyclic protocol for detecting ODMR in a continuous-wave regime included stages of 1) continuous excitation by 532 nm laser; 2) two detecting windows; and 3) MW excitation pulses (indicated with red, green, and blue colors in Fig. S3a). The detecting windows were implemented with two counters connected to a SPAD through a t-adapter. The reference ("detector-ref", 0.03 – 0.47 ms) and signal ("detector-signal", 0.53 – 0.97 ms) time windows corresponded to the conditions when MWs were ON and OFF, respectively. MW pulses were applied in a time period of 0.52 – 0.98 ms and were controlled by a MW switch. The MW frequency was swept in the range from 2820 to 2920 MHz with a step of 10 MHz. At each frequency step the measurement cycle was repeated 10000 and 60000 times for ND (area "C" in Fig. 4a of the main manuscript) and VG far end (area "B" in Fig. 4a of the main manuscript) signals, correspondingly.

Pulsed ODMR

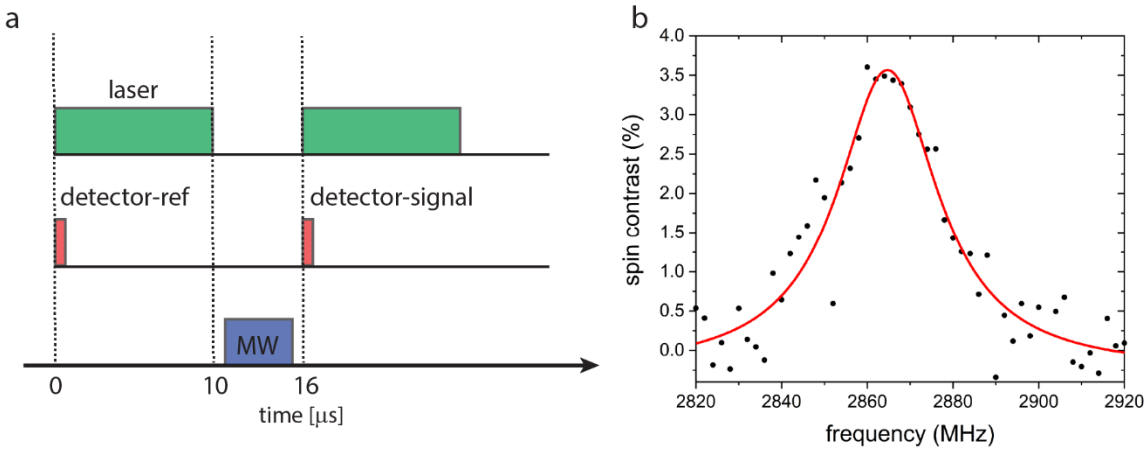

Figure S4. (a) Pulsed ODMR measurement protocol. (b) Spin contrast curve obtained in a pulsed ODMR experiment with a 4 μs MW pulse at 8 dBm generator power.

We also performed ODMR experiment in a pulsed regime, where optical pumping and MW excitations separately affected the NV ensemble. The NV ensemble inside the v-groove was interrogated with a pulsed sequence illustrated in Fig. S4a. The sequence consisted of 10 μs initializing laser pulses followed by 4 μs MW excitation pulses ($t_{MW} >> T_2^* \sim 0.1$ μs[1]). NV fluorescence was detected within 0.3-μs-long time windows, synchronized with the beginning of the laser pulses.

III. Microwave B-field delivery

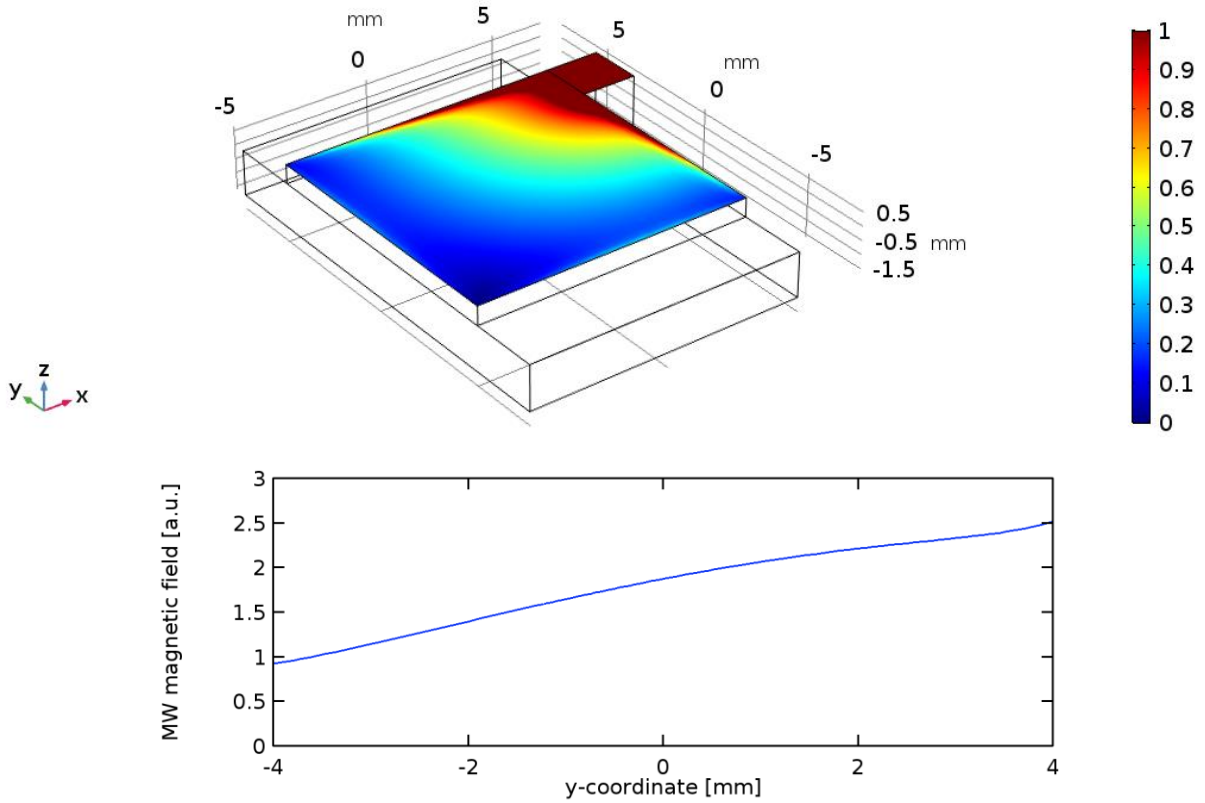

Figure S5. Simulated MW (2.87 GHz) H-field distribution on 10 × 10 mm^2 sample surface. The estimated gradient of the field magnitude is about ±5% per 1 mm in arbitrary direction.

We performed additional measurements to quantify the delivered microwave power. First, to numerically estimate the power reaching the sample, we measured losses in SMA cables, connectors and the microwave switch (ZFSWA2-63DR+). According to our estimates, about 10 Watts enter the sample, of which we assume 10% to be transmitted to the metallic film. This power of 1 W was fed through the lumped port in COMSOL simulations, from which the estimated in-plane B-field amplitude is approximately 1 G, leading to an upper bound on Rabi frequency of $2\pi \times 3$MHz.

IV. Pump filtering with a v-groove collector

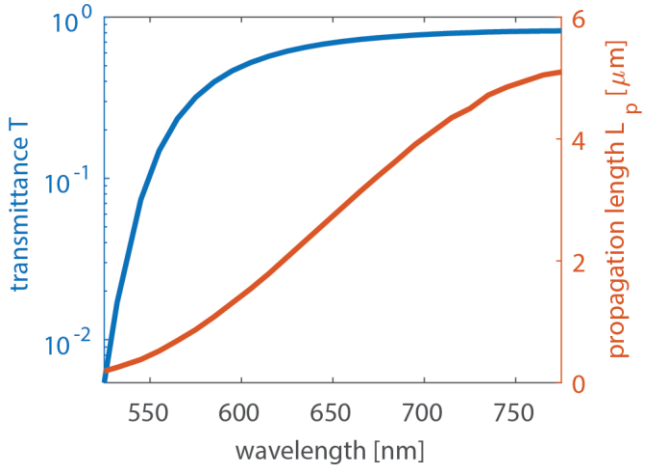

Figure S6. Calculated wavelength dependencies of the v-groove fundamental mode propagation length (orange) and collector transmittance at the propagation distance of 1 μm (blue). Demonstrated v-groove can be used as a long pass filter for cutting off the pump at 532 nm.

V. Heating effect associated with microwave delivery

To investigate the significance of the heating effect associated with microwave delivery, we recorded the ODMR curves in the pulsed experiment (see Fig. S4a) at various MW powers and plotted the power dependence of ODMR central frequency (see Fig. S7). Fitting of the data showed that the ODMR central frequency shifted by less than 3 MHz towards lower frequencies. Assuming that the temperature derivative of crystal field splitting (dD/dT) is on the order of -100 kHz/K^2, then the nanodiamond should experience temperature increase of about 30°C at maximum MW power. Therefore, we conclude that the demonstrated microwave delivery does not produce a significant heating effect.

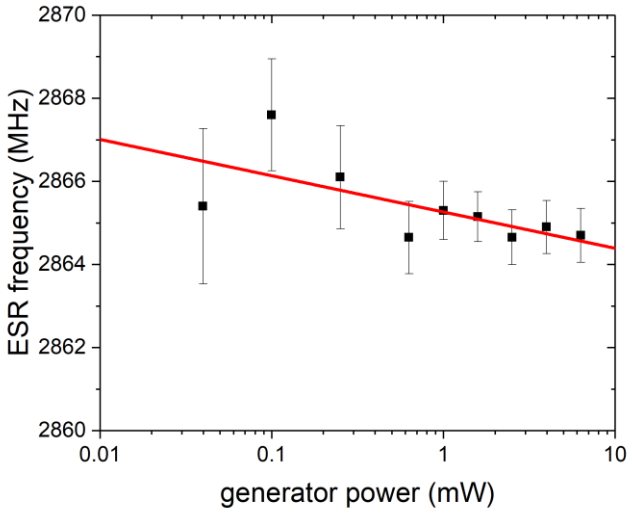

Figure S7. ODMR frequency vs MW generator output power for a nanodiamond NV ensemble sitting on top of the metallic v-groove.

References

(1) Acosta, V. M.; Bauch, E.; Ledbetter, M. P.; Santori, C.; Fu, K.-M. C.; Barclay, P. E.; Beausoleil, R. G.; Linget, H.; Roch, J. F.; Treussart, F.; Chemerisov, S.; Gawlik, W.; Budker, D. Diamonds with a High Density of Nitrogen-Vacancy Centers for Magnetometry Applications. *Phys. Rev. B* **2009**, *80* (11), 115202.

(2) Toyli, D. M.; Christle, D. J.; Alkauskas, A.; Buckley, B. B.; Van de Walle, C. G.; Awschalom, D. D. Measurement and Control of Single Nitrogen-Vacancy Center Spins above 600 K. *Phys. Rev. X* **2012**, *2* (3), 031001.